Peng *et al.*
Chinese Journal of Mechanical Engineering (2021) 34:113
https://doi.org/10.1186/s10033-021-00634-8

Chinese Journal of Mechanical Engineering

ORIGINAL ARTICLE

Open Access

Effect of Deformation on Microstructure and Mechanical Properties of Medium Carbon Steel During Heat Treatment Process

Yan Peng*, Caiyi Liu and Ningning Wang

Abstract

The current research of the Q-P and Q-P-T process has been focused on controlling the heating temperature and holding time, or adding alloy elements into the steel to induce precipitation strengthening and improve the strength and plasticity of the steel. In this article, based on a quenching-partitioning-tempering (Q-P-T) process combined with a hot deformation technology, a deforming-quenching-partitioning-tempering (D-Q-P-T) process was applied to medium carbon steel. The effect of the heat treatment parameters on the microstructure and mechanical properties of experimental steel under deformation was studied. Through use of a scanning electron microscope (SEM), transmission electron microscopy (TEM) and tensile tests, the optimal heat treatment conditions for realizing high strength and plasticity that meet the safety requirements were obtained. The mechanism for the D-Q-P-T process to improve the strength and plasticity of experimental steel was discussed. A multiphase composite structure of lath martensite and retained austenite was obtained. Compared with the Q-P-T process, use of the D-Q-P-T process can increase the strength of steel by 57.77 MPa and the elongation by 5%. This study proposes a method to improve the strength and plasticity of steel.

Keywords: Deforming-quenching-partitioning-tempering, Microstructure, Mechanical properties, Product of strength and ductility ($R_m \times A$)

1 Introduction

High-strength steel plays an important role in realizing lightweight automobiles with improved safety performance. Dual-phase (DP) steel and transformation-induced plasticity (TRIP) steel present a good combination of strength (500–1000 MPa) and elongation (15%–40%) in comparison with conventional high strength low alloy (HSLA) steels [1–5]. Research data show that the application of high-strength steel can reduce the thickness of 1.0–1.2 mm body panels to 0.7–0.8 mm. In addition, the body mass can be reduced by 15%–20%, which can lead to fuel savings of 8%–15% [6–9]. Based on the above strong points, high-strength steel is widely used in automobile manufacturing and other fields. At present, the development of high-strength steel is directed towards improving strength and plasticity. Advanced high-strength steel heat treatment technology has become a research hotspot [10–15].

To achieve a higher strength, a heat treatment process designated quenching and partitioning (Q-P) process has recently been proposed by Speer et al. [16–18]. The Q-P process includes heating medium carbon steel to the austenitic zone for heat preservation, then quenching to a certain temperature between the martensite-start (M_s) and martensite-finish (M_f) temperatures. The steel is then held at a temperature either at (I step process) or above (II step process) the initial quenching temperature (Figure 1(a)), or cooled non-isothermally at a slow rate to below the initial quenching temperature for hot-rolled sheet steel processing (Figure 1(b)). Carbon is permitted to partition

*Correspondence: pengyan@ysu.edu.cn
National Engineering Research Center for Equipment and Technology of Cold Rolled Strip, Yanshan University, Qinhuangdao 066004, China

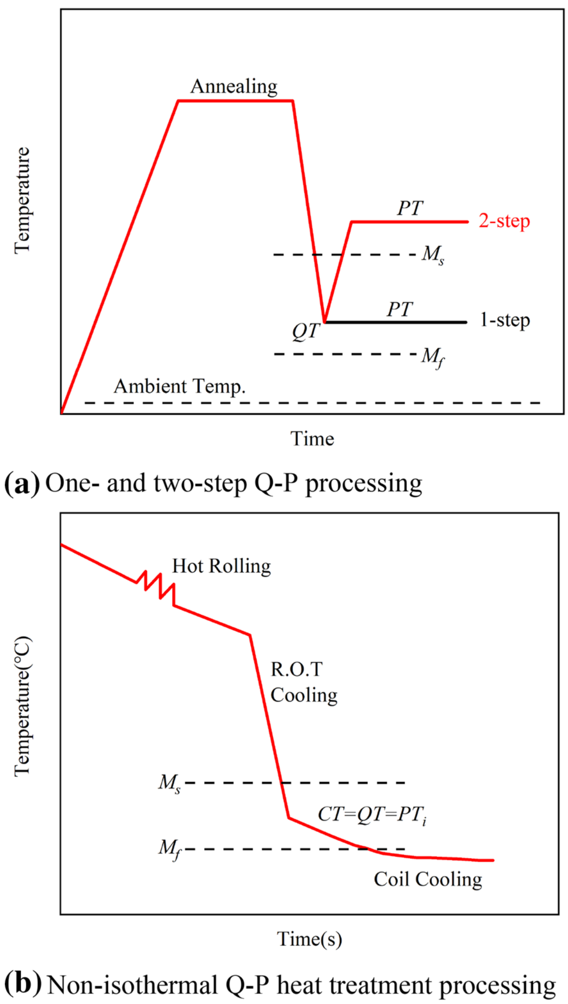

Figure 1 Schematics for conventional heat treatment

from supersaturated partially transformed martensite into retained austenite. The microstructure is martensite and retained austenite, which can improve the strength and toughness of the steel. Recently, many studies show that the precipitation of second-phase particles has a positive impact on the mechanical properties of the material [19, 20]. Consider the influence of the precipitation behaviour of alloy elements after this process on the structure and properties. Hsu et al. [21, 22] proposed a novel heat treatment method, namely, a quenching-partitioning-tempering (Q-P-T) process. Compared with the Q-P process, carbide former elements (such as Nb, Mo and V) are added into Q-P-T steels to form fine stable carbides during the partitioning process so as to strengthen steels. A lot of research has been executed since the Q-P-T process was developed [23–25]. At present, most of the research on the Q-P and Q-P-T process has been focused on controlling the heating temperature and holding time, or adding alloy elements into the steel to induce precipitation strengthening and improve the strength and plasticity of the steel. In addition to precipitation strengthening, fine grain strengthening is also an important factor to improve the strength and plasticity of steel [26–30]. Therefore, a mechanism for deformation fine grain strengthening is proposed in this paper. By introducing a deformation process before the Q-P-T process, the D-Q-P-T process was proposed to improve the comprehensive mechanical properties of steel.

2 Materials and Methods

The chemical composition of the experimental steel is listed in Table 1, together with A_{c3}, M_s, M_f temperatures and the critical cooling rate, which were determined by a Gleeble-3800 thermal simulator, as shown in Figure 2 and Figure 3. It can be seen from the figures that the A_{c3} temperature is 800 °C, M_s is 385 °C, and M_f is 195 °C. The experimental temperature control was formulated according to the tested critical transition temperatures.

Round bar specimens with a length of 75 mm and diameter 15 mm were cut from the steel plate for compressive deformation. Three groups of experiments were designed. The first group of experiments aimed to compare D-Q-P-T with the Q-P-T process and analyze the effect of deformation on the microstructure and mechanical properties of the heat-treatment process. In the D-Q-P-T experiment, a Gleeble-3800 thermal simulator was used to heat the samples to 950 °C for 5 min, followed by air cooling to 870 °C for 10 s; the samples were then subject to a compression of 60% and quenching to 300 °C for 10 s, followed by tempering at 400 °C for 10 s, and, finally, water quenching to room temperature. The Q-P-T process does not undergo deformation treatment. Other heat treatment process parameters were the same as those used for the D-Q-P-T process. The experimental scheme is shown in Figure 4. The second group of experiments aimed to analyze the effect of different quenching temperatures for the D-Q-P-T process on the microstructure and mechanical properties. The quenching temperature was 250 °C, 300 °C

Table 1 Chemical composition of the steel (wt%)

C	Si	Mn	Cr	Ni	S	P	Cr
0.41	0.24	0.58	0.88	0.014	0.006	0.023	0.88

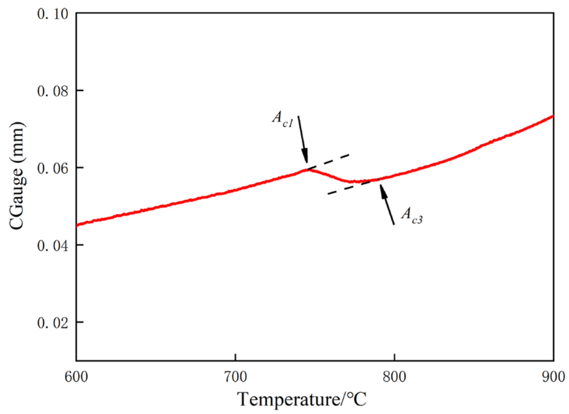

Figure 2 Austenitic thermal expansion curve

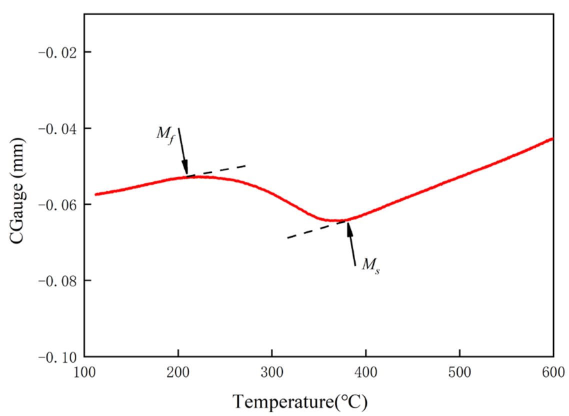

Figure 3 Martensite thermal expansion curve

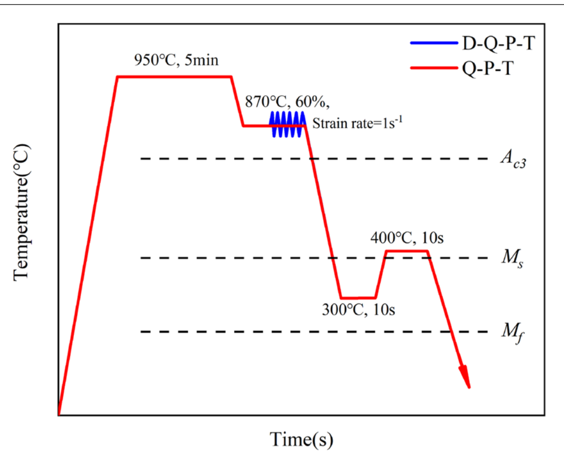

Figure 4 The first group of experiments

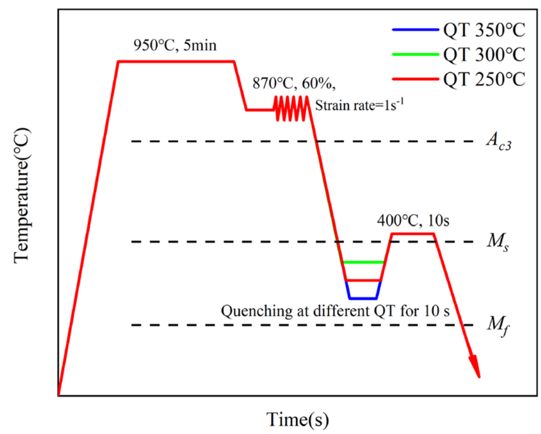

Figure 5 The second group of experiments

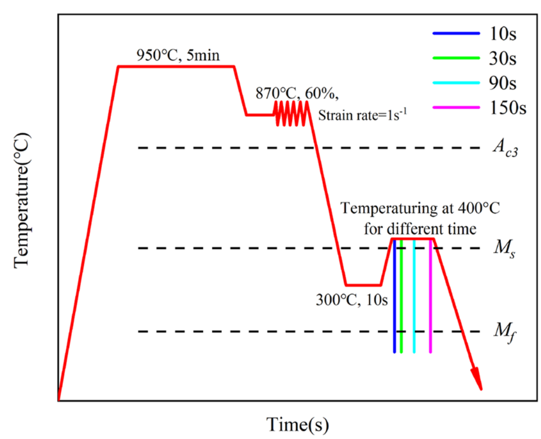

Figure 6 The third group of experiments

and 350 °C for 10 s. Other heat treatment process parameters were the same as those used for the first group of experiments, as shown in Figure 5. The third group of experiments aimed to study the effect of different tempering times for the D-Q-P-T process on the microstructure and mechanical properties. Samples were tempered at 400 °C for 10 s, 30 s, 90 s and 150 s, respectively. Other heat treatment process parameters were the same as those used in the first group of experiments, as shown in Figure 6.

To observe the microstructure changes for the three groups, the samples were cut, ground and polished, and then corroded with a detergent solution of saturated picric acid and 3% nital solution before using Optical Microscopy (OM) to observe the microstructure. To clearly observe the morphology of the precipitate, a 0.5 mm thickness sheet was cut by a molybdenum wire cutting machine, which was then ground and polished to a thickness of approximately 50 μm. The morphology of the precipitate was observed by a scanning electron microscope (SEM) and transmission electron microscopy (TEM). To test the mechanical properties, the sample was processed into a tensile sample, as shown in Figure 7. The sample was stretched at a speed of 0.02 mm · min^{-1} to obtain the tensile strength and elongation under different experimental schemes.

3 Results and Discussion

3.1 Microstructure

Optical micrographs of the specimens prepared under the deforming-quenching and quenching processes are shown in Figure 8 [31]. It can be seen from the figure that the grain size for the deforming-quenching process is large; for the deforming-quenching process, due to the deformation before the quenching process, with the influence of high temperature and large deformation, the sample shows dynamic recrystallization, which makes the grain refined and increases the dislocation density. Therefore, compared with the quenching process, the grain size for the deforming-quenching process is significantly smaller.

To further observe the D-Q-P-T and Q-P-T processes microstructure, the experimental steel was analyzed by SEM, as shown in Figure 9 [31]. The D-Q-P-T process is shown in Figure 9(a). It is clear that the microstructural feature of these D-Q-P-T samples is typical lath martensite, and the lath martensite is fractured. Compared with the Q-P-T process, the D-Q-P-T process can refine grains and increase the dislocation density, as shown in Figure 9(b). The dynamic recrystallization absorption for the D-Q-P-T process takes place in the process of deformation to eliminate some dislocations. However, most of the dislocations are inherited by the generated martensite structure, and, finally, the lath martensite and retained austenite structures with high dislocation density are obtained, which indicates that the deformation takes place before the Q-P-T process can affect the refining of grains.

Figure 10 shows SEM micrographs for samples quenched at a temperature of 250 °C, 300 °C and 350 °C. Figure 10(a) shows the SEM micrograph for a sample quenching temperature of 250 °C. The microstructure is lath martensite, and the laths are intertwined; a large number of lath structures are combined into martensite

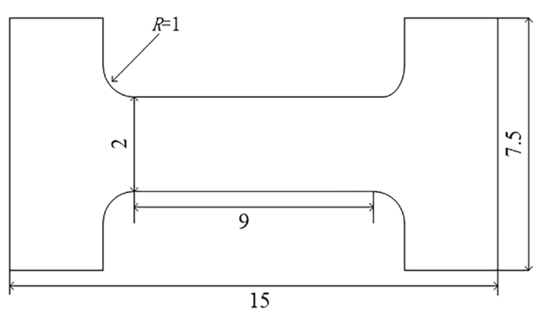

Figure 7 Dimension of the tension sample (mm)

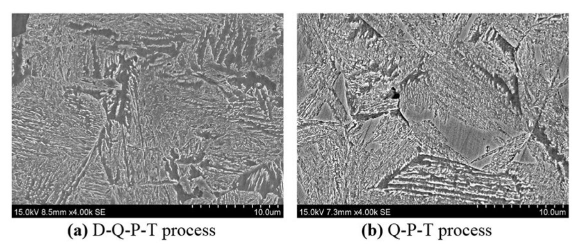

Figure 9 SEM micrographs of the D-Q-P-T and Q-P-T samples [31]

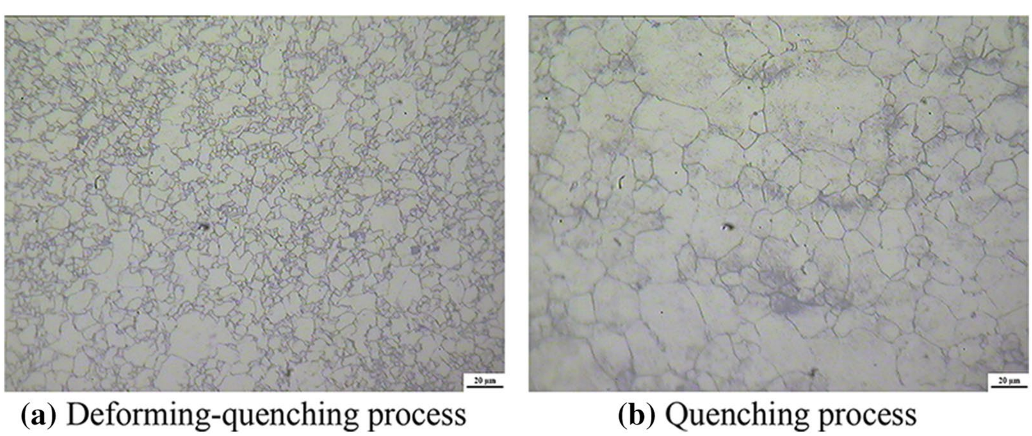

Figure 8 Optical micrographs of the D-Q-P-T and Q-P-T samples [31]

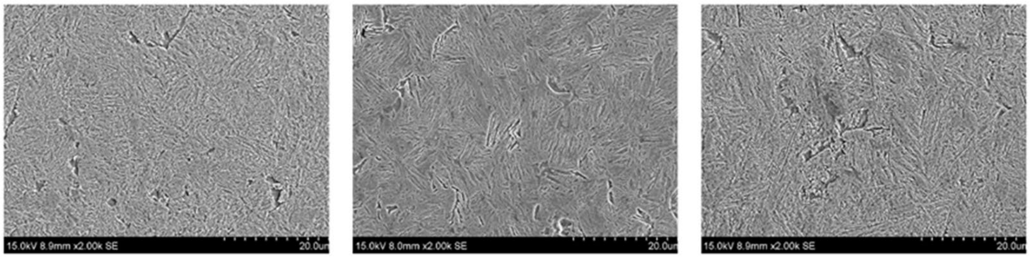

(a) 250 ℃ (b) 300 ℃ (c) 350 ℃

Figure 10 SEM micrographs of the D-Q-P-T samples prepared at different quenching temperatures

bundles. The lath bundles of martensite are zigzag and curved, which is due to the deformation; in addition, a small amount of feathery bainite structure is found between the martensite bundles. At a quenching temperature of 300 °C, it can be seen from Figure 10(b) that the martensite bundle is more obvious. For a quenching temperature of 350 °C, as shown in Figure 10(c), the martensite is relatively coarse. With increasing quenching temperature, the lath martensite becomes coarser, with many dislocations and twist breaks between the laths. This is because the experimental steel is first deformed in the austenitized zone before the Q-P-T process, and the austenite grains are elongated during the deformation process. As the amount of deformation accumulates, the grain boundary becomes tortuous or even fractured. High dislocation density results in a larger grain boundary area, smaller grain size and higher dislocation density, which are inherited by the later martensite.

Figure 11 shows TEM micrographs for D-Q-P-T samples prepared with different quenching temperatures. It can be seen from the figure that the lath martensite fractures and bends, which further confirms that the deformation increases the dislocation density. When the quenching temperature is 250 °C, as shown in Figure 11(a), the lath martensite is narrow, and the average width of the lath martensite is 150 nm, and the average width of the retained austenite is 25 nm. When the quenching temperature is 300 °C, as shown in Figure 11(b), it can be seen that the martensite lath becomes thicker, and the average width of the lath martensitic is 250 nm. With increasing quenching temperature, the average width of the retained austenite is 80 nm. It can be seen that the dislocation density is high at the quenching temperature of 350 °C, as shown in Figure 11(c). The average width of the retained austenite is larger; the channels for carbon atom diffusion increase due to the high dislocation density. With increasing quenching temperature, the diffusion of carbon atoms accelerates, resulting in the diffusion of more carbon atoms to the retained austenite. However, due to the short tempering time, which is only 10 s, the retained austenite cannot fully accumulate and grow, leading to the retained austenite to exhibit different lengths and distributions.

From the above analysis, it is known that the tempering time also affects the microstructure. Therefore, the selection of an appropriate tempering time is also a key factor in the D-Q-P-T process. Figure 12 shows SEM micrographs for samples prepared using different tempering times of 10 s, 30 s, 90 s and 150 s at 400 °C. It can be seen from Figure 12 that the microstructure is martensitic

(a) 250 ℃ (b) 300 ℃ (c) 350 ℃

Figure 11 TEM micrographs of D-Q-P-T samples prepared using different quenching temperatures

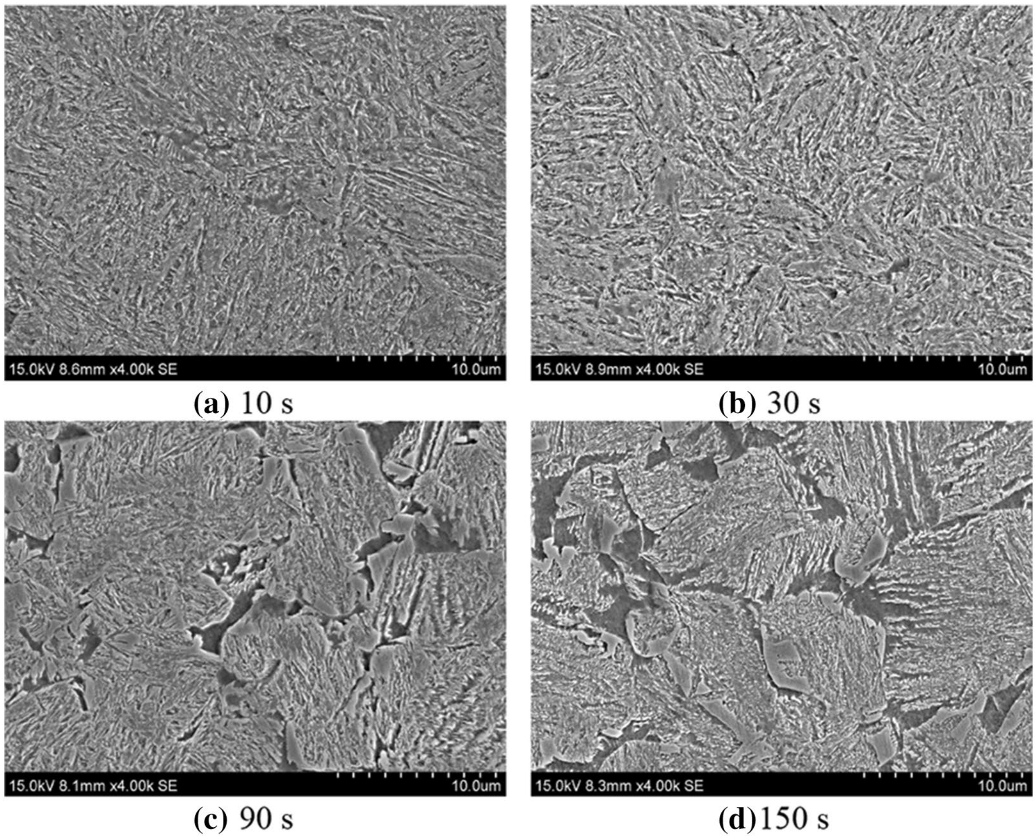

Figure 12 SEM micrographs of D-Q-P-T samples prepared using different tempering time

under different tempering times. When the tempering time is 10 s and 30 s, as shown in Figure 12(a), (b), the size of martensite laths is smaller. With increasing tempering time, as shown in Figure 12(c), (d), the size of martensite laths increases.

Figure 13 shows TEM micrographs for D-Q-P-T samples prepared with different tempering times. When the tempering time is 10 s, as shown in Figure 13(a), the lath martensite structure can be seen clearly in the figure, and there is a high dislocation density. The retained austenite is distributed between the lath martensite. Due to the short tempering time of only 10 s, the carbon atoms in the martensite cannot be fully diffused into the retained austenite, resulting in less content and a shorter width of 20–23 nm for the retained austenite. When the tempering time is 30 s, as shown in Figure 13(b), one observes that the retained austenite becomes wider and longer. When the tempering time is 90 s, as shown in Figure 13(c), (d), the amount of retained austenite is observed to decrease, which is due to the transformation of retained austenite into martensite or bainite with increasing tempering time. As a result, the retained austenite content is reduced. In Figure 13(e), the SAED pattern analysis indicates the presence of retained austenite together with martensite.

In the D-Q-P-T process, the retained austenite can be stable in existence. On the one hand, due to the first quenching temperature between M_s and M_f in the Q-P-T process, part of the austenite will remain after the first quenching, and carbon atoms will diffuse from the martensite to the remained austenite after tempering, thus forming a part of the carbon-rich austenite, which will exist stably. On the other hand, due to the deformation, the microstructure is refined, and the interaction between martensite and retained austenite leads to the microstructure to restrict each phase, so that the austenite remains stable.

3.2 Mechanical Properties

The comparison of mechanical properties for samples prepared using the D-Q-P-T and Q-P-T process is shown in Table 2 [31]. Compared with the Q-P-T process, the tensile strength of a sample prepared using the D-Q-P-T process is increased by 57.77 MPa and the elongation is also improved. There is deformation before Q-P-T heat treatment process, which can refine the grains and

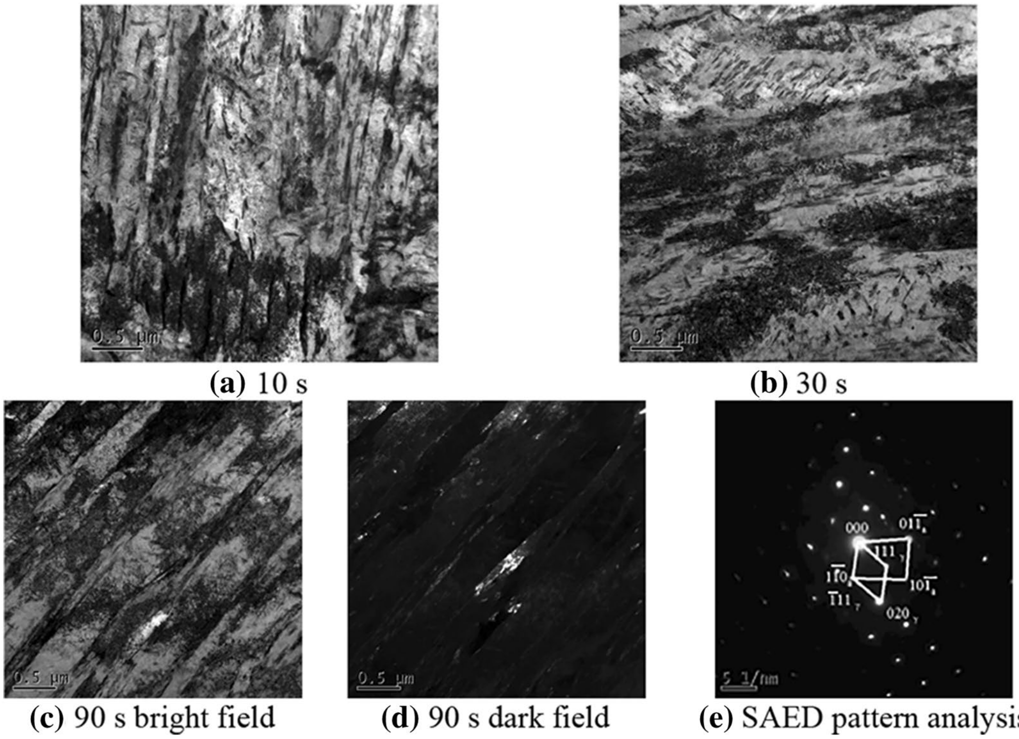

Figure 13 TEM micrographs of D-Q-P-T samples prepared with different tempering times

Table 2 Mechanical properties for D-Q-P-T and Q-P-T [31]

Process	Properties		
	Tensile strength (MPa)	Elongation (%)	$R_m \times A$ (GPa%)
D-Q-P-T	1388.22	17.72	24.6
Q-P-T	1330.45	13.64	18.15

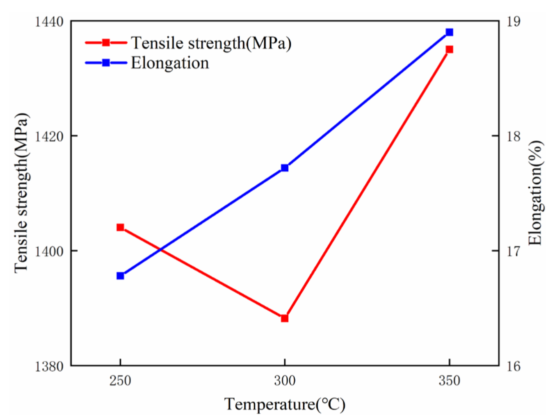

Figure 14 Tensile strength and elongation with different quenching temperatures

increase the strength and plasticity of the experimental steel. On the one hand, the grain size obtained in the D-Q-P-T process is relatively small due to the effect of deformation, which plays an important role in improving the strength and plasticity of the experimental steel. On the other hand, a large number of dislocations will be produced during deformation, which will increase the number of channels for carbon atom diffusion, resulting in more retained austenite content in the D-Q-P-T process than in the Q-P-T process. This will improve the comprehensive mechanical properties of the material.

Figure 14 shows the tensile strength and elongation of the experimental steel at different quenching temperatures. It can be seen from the figure that the tensile strength decreases first and then increases with increasing quenching temperature, while the elongation increases throughout. When the quenching temperature is 350 °C, the tensile strength is 1435 MPa and the elongation is 18.9%. The tensile strength of the experimental steel obtained by the D-Q-P-T process reaches above 1350 MPa, and the elongation exceeds 16%. The change trend for the elongation also reflects the fact that the content of retained austenite in the soft phase increases with increasing quenching temperature.

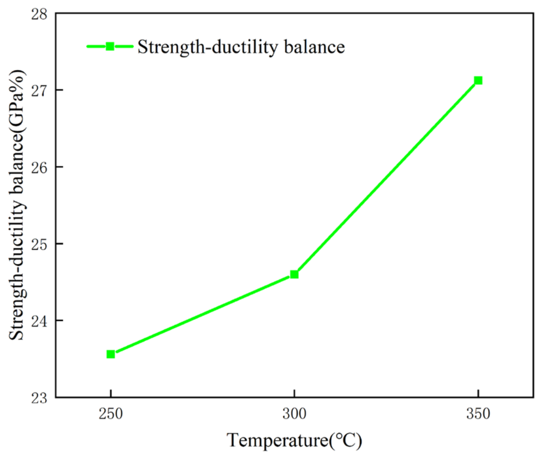

Figure 15 Strength and ductility with different quenching temperatures

Figure 15 shows the change in the strength and ductility ($R_m \times A$) of the experimental steel. Under different quenching temperatures, the change in the strength and ductility increases with increasing quenching temperature. The strength and ductility of the experimental steel obtained through the D-Q-P-T process reaches above 23 GPa%. The highest value of 27.1 GPa% is obtained for a quenching temperature of 350 °C. This is because the strength and toughness of the experimental steel after the D-Q-P-T process will have a blending process. The final microstructure obtained under different quenching temperatures involves a process of mutual distribution of hard and soft phases.

Figure 16 shows the tensile strength and elongation of the experimental steel at different tempering times. It can be seen from Figure 16 that the tempering time has an influence on the mechanical properties of the steel. With the extension of the tempering time, the tensile strength first increases and then decreases. When the tempering time is 30 s, the maximum tensile strength of the experimental steel is 1487.5 MPa. With increasing tempering time, the martensite morphology of the experimental steel becomes uniform and coarse. The martensite microstructure will decompose into ferrite and carbide, which will affect the mechanical properties of the material. The elongation of the experimental steel reaches above 16.5% at different tempering times. Under this heat treatment, the microstructure of the experimental steel contains more retained austenite. During the stretching process, the retained austenite belongs to the soft phase, and the martensite is the hard phase. The coordination between the hard phase and the soft phase plays an important role in improving the toughness of the experimental steel.

Figure 17 shows the change in the strength and ductility ($R_m \times A$) of the experimental steel. It can be seen from the figure that the strength and ductility is different at different tempering times. When the tempering time is 30 s, the maximum strength and ductility of the experimental steel is 27.1 GPa%. Due to the deformation in the austenite zone, grain refinement occurs. After the subsequent heat treatment, the martensite, bainite and retained austenite are finally obtained. Such composite microstructures can not only increase the strength of the steel, but also enhance the toughness of the steel. The experimental steel has a high product for the strength and ductility ($R_m \times A$).

3.3 D-Q-P-T Strengthening Mechanism

For the strengthening mechanism of the material, fine grain strengthening can improve the strength and toughness of the material at the same time. The grain refinement process for the D-Q-P-T process can be divided

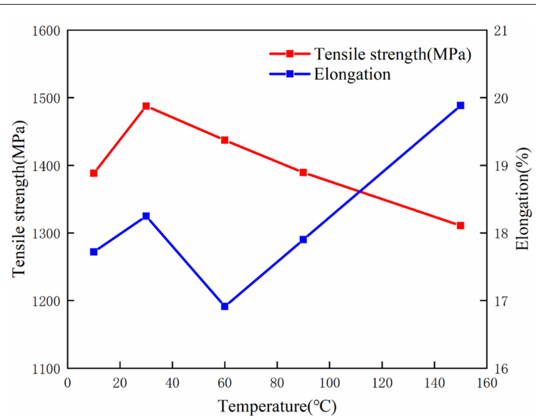

Figure 16 Tensile strength and elongation with different tempering times

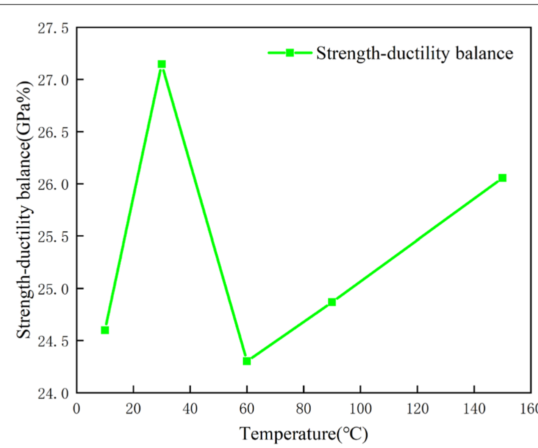

Figure 17 Strength and ductility with different tempering times

into the following stages: deformation of the austenite zone leads to a large angle change in the grain boundary. At the initial stage of deformation, the austenite grain boundary bends, and there is a stress effect between the grain boundaries, which increases the dislocation density. The sub-grain boundary appears under the stress. If the deformation continues to increase, it will lead to a non-uniform distribution of grain boundary strain. This non-uniform strain distribution causes the grain boundary to have tangential strain, which causes the grain boundary to move abnormally. With increasing deformation, the strain further accumulates, and the grain boundary produces large bending and recrystallization behaviour occurs. In the D-Q-P-T process, the martensite nucleates at the refined grain boundary. Due to the effect of deformation, high dislocation density will hinder the growth of martensite, thereby refining the martensite microstructure and increasing the strength of the experimental steel.

4 Conclusions

(1) In this paper, deformation is introduced into the heat-treatment process for an experimental steel. Dynamic recrystallization behavior is observed for the material due to the deformation in the high temperature austenite zone. Because the material thermomechanical process integrates deformation–quenching–partitioning-tempering, the grain can be refined, and finally, a high dislocation density lath martensite and retained austenite can be obtained, which plays an important role in improving the tensile strength and elongation of the experimental steel.

(2) In this paper, Fe-0.41C-0.24Si-0.58Mn-0.88Cr-0.014Ni (wt%) steel was treated by a D-Q-P-T process, and optimized heat treatment parameters were obtained. The maximum strength and ductility of the experimental steel was determined to be 27.1 GPa%.

(3) The D-Q-P-T process was used to obtain an experimental steel with a tensile strength of 1388.22 MPa, elongation of 17.72%, and a strength and ductility of 24.6 GPa%. For the Q-P-T process, the experimental steel shows a tensile strength of 1330.45 MPa, elongation of 13.64%, and a strength and ductility of 18.15 GPa%. Compared with the Q-P-T process, the D-Q-P-T process improves the tensile strength of the experimental steel by 57.77 MPa, and the elongation is also significantly improved. The D-Q-P-T process proposed in this paper can be used to simultaneously improve the strength and ductility.

(4) When the quenching temperature for the D-Q-P-T process is 250 °C, 300 °C or 350 °C, the maximum tensile strength of the experimental steel is 1435 MPa, the elongation is 18.9%, and the strength and ductility is 27.1 GPa%.

(5) For a tempering time of 10 s, 30 s, 90 s or 150 s for the D-Q-P-T process, the tensile strength ranges from 1310.66–1487.48 MPa, the elongation ranges from 16.91%–19.88%.

(6) In this paper, a design idea for preparing a multiphase microstructure for steel is realized. The experimental steel microstructure is composed of lath martensite and retained austenite. The existence of a multiphase microstructure not only enhances the strength of the experimental steel but also increases the plasticity of the experimental steel, which improves the strength and ductility.

Acknowledgements
Not applicable.

Authors' Contributions
YP and NW were in charge of the whole trial; CL and NW wrote the manuscript; CL and NW assisted with sampling and laboratory analyses. All authors read and approved the final manuscript.

Authors' Information
Yan Peng is a professor at *School of Mechanical Engineering, Yanshan University, China*. His research interests include continuous strip rolling equipment-technology-product flexible adaptation and multi-objective synergistic control under instantaneous mutation.
Caiyi Liu is a PhD candidate at *School of Mechanical Engineering, Yanshan University, China*. His research interests include materials characterization and mechanical properties during flexible rolling process.
Ningning Wang is a master candidate at *School of Mechanical Engineering, Yanshan University, China*. His research interests include static recrystallization during flexible rolling process.

Funding
Supported by Regional Joint Funds of National Natural Science Foundation of China (Grant No. U20A20289).

Competing Interests
The authors declare no competing financial interests.

Received: 31 May 2020 Revised: 28 January 2021 Accepted: 2 November 2021
Published online: 27 November 2021

References

[1] S P Qu, Y C Zhang, X Pang, et al. Influence of temperature field on the microstructure of low carbon microalloyed ferrite–bainite dual-phase steel during heat treatment. *Materials Science and Engineering: A*, 2012, 536: 136-142.
[2] L Ding, J P Lin, J Y Min, et al. Necking of Q&P steel during uniaxial tensile test with the aid of DIC technique. *Chinese Journal of Mechanical Engineering*, 2013, 26: 448-453.
[3] E Shafiei, K Dehghani. Effects of thickness ratio and length of thickness transition zone on the tensile behavior of tailor rolled blanks. *Transactions of the Indian Institute of Metals*, 2018, 71(5): 1211-1222.

[4] S J Zhang, X H Liu, L Z Liu. A tensile specimen of tailor rolled blanks with equal probability in yield and its mechanical behavior analysis. *Materials*, 2018, 11(5): 693.
[5] Z S Mandana, B Silvia, G Andrea, et al. Impact of warm rolling process parameters on crystallographic textures, microstructure and mechanical properties of low-carbon boron-bearing steels. *Metals*, 2018, 8(11): 927.
[6] L Kong, C Y Liu, Y Peng. Study on variable gradient characteristics hot stamping under non-uniform temperature field. *Journal of Mechanical Engineering*, 2017, 53(8): 75-81. (in Chinese)
[7] Y Peng, C Y Liu, L H Hao, et al. Review of performance gradient distribution hot forming technology. *Journal of Mechanical Engineering*, 2016, 52(8): 67-75. (in Chinese)
[8] X D Li, S Han, C Y Wang, et al. Research on the warm-hot forming process and its performance evaluation for the third-generation automobile steel. *Journal of Mechanical Engineering*, 2017, 53(8): 35-42. (in Chinese)
[9] L Ying, B F Zhang, M H Dai, et al. Optimization of crashworthiness for tailored hot forming b-pillar based on side impact. *Journal of Mechanical Engineering*, 2017, 53(12): 102-109. (in Chinese)
[10] Y Chen, H Zhang, J J Tang, et al. Integrated modelling of microstructure evolution and mechanical properties prediction for Q&P hot stamping process of ultra-high strength steel. *Chinese Journal of Mechanical Engineering*, 2020, 33: 45.
[11] F X Ding, L F Lan, Y J Yu, et al. Experimental study of the effect of a slow-cooling heat treatment on the mechanical properties of high strength steels. *Construction and Building Materials*, 2020, 241: 118020.
[12] Z J Xie, G Han, W H Zhou, et al. A novel multi-step intercritical heat treatment induces multi-phase microstructure with ultra-low yield ratio and high ductility in advanced high-strength steel. *Scripta Materialia*, 2018, 155: 164-168.
[13] L Fan, T L Wang, Z B Fu, et al. Effect of heat-treatment on-line process temperature on the microstructure and tensile properties of a low carbon Nb-microalloyed steel. *Materials Science and Engineering: A*. 2014, 607: 559-568.
[14] S Zhang, X Hu, C Niu, et al. Annealing of HC340LA tailor rolled blanks—Control of mechanical properties and formability. *Journal of Materials Processing Technology*, 2020, 281: 116581.
[15] P Dinesh Babu, P Gouthaman, P Marimuthu. Effect of heat sink and cooling mediums on ferrite austenite ratio and distortion in laser welding of duplex stainless steel 2205. *Chinese Journal of Mechanical Engineering*, 2019, 32: 50.
[16] J Speer, D K Matlock, B C De Cooman, et al. Carbon partitioning into austenite after martensite transformation. *Acta Materialia*, 2003, 51(9): 2611-2622.
[17] J G Speer, D V Edmonds, F C Rizzo, et al. Partitioning of carbon from supersaturated plates of ferrite, with application to steel processing and fundamentals of the bainite transformation. *Current Opinion in Solid State and Materials Science*, 2004, 8(3-4): 219-237.
[18] F L H Gerdemann, J G Speer, D K Matlock. Microstructure and hardness of steel grade 9260 heat-treated by the quenching and partitioning (Q&P) process. *Materials Science and Technology*, 2004, 1: 439-449.
[19] H L Yi, P Chen, Z Y Hou, et al. A novel design: Partitioning achieved by quenching and tempering (Q–T & P) in an aluminium-added low-density steel. *Scripta Materialia*, 2013, 68(6): 370-374.
[20] J G Speer, E De Moor, K O Findley, et al. Analysis of microstructure evolution in quenching and partitioning automotive sheet steel. *Metallurgical and Materials Transactions A*, 2011, 42(12): 3591.
[21] T Y Hsu, Z Y Xu. Design of structure, composition and heat treatment process for high strength steel. *Materials Science Forum*, 2007, 561: 2283-2286.
[22] X D Wang, N Zhong, Y H Rong, et al. Novel ultrahigh-strength nanolath martensitic steel by quenching–partitioning–tempering process. *Journal of Materials Research*, 2009, 24(1): 260-267.
[23] N Zhong, X D Wang, L Wang, et al. Enhancement of the mechanical properties of a Nb-microalloyed advanced high-strength steel treated by quenching–partitioning–tempering process. *Materials Science and Engineering: A*, 2009, 506(1-2): 111-116.
[24] S Zhou, K Zhang, Y Wang, et al. High strength-elongation product of Nb-microalloyed low-carbon steel by a novel quenching–partitioning–tempering process. *Materials Science and Engineering: A*, 2011, 528(27): 8006-8012.
[25] X D Tan, D Ponge, W J Lu, et al. Carbon and strain partitioning in a quenched and partitioned steel containing ferrite. *Acta Materialia*, 2019, 165: 561-576.
[26] K M Xue, Z Wang, M Liu, et al. Effect of high-pressure torsion on microstructure and properties of TA 15 Titanium alloy. *Rare Metal Materials and Engineering*, 2019, 48(4): 1189-1194.
[27] C Li, L Huang, M Zhao, et al. Influence of hot deformation on dynamic recrystallization behavior of 300M steel: Rules and modeling. *Materials Science and Engineering: A*, 2020, 797: 139925.
[28] C Zhang, L Zhang, Q Xu, et al. The kinetics and cellular automaton modeling of dynamic recrystallization behavior of a medium carbon Cr-Ni-Mo alloyed steel in hot working process. *Materials Science and Engineering: A*, 2016, 678: 33-43.
[29] Y H Mozumder, K A Babu, R Saha, et al. Dynamic microstructural evolution and recrystallization mechanism during hot deformation of intermetallic-hardened duplex lightweight steel. *Materials Science and Engineering: A*, 2020, 788: 139613.
[30] G He, F Liu, L Huang, et al. Controlling grain size via dynamic recrystallization in an advanced polycrystalline nickel base superalloy. *Journal of Alloys and Compounds*, 2017, 701: 909-919.
[31] Y Peng, C Y Liu, N N Wang, et al. Effect of a novel heat treatment process on microstructure and mechanical properties of medium carbon steel. Iron and Steel, 2021, 56: 85-89.